Hydrodynamic calculation of the frequency dependent friction on the bond of a diatomic molecule

B. Mishra and B. J. Berne
Department of Chemistry and Center for Biomolecular Simulations, Columbia University, New York, New York 10027

(Received 17 November 1994; accepted 12 April 1995)

In this paper molecular hydrodynamics is used to calculate the dynamic friction on the intramolecular vibrational coordinate of a homonuclear diatomic molecule dissolved in a simple liquid. The predicted dynamic friction is then compared to recent computer experiments. Agreement with the experimental dynamic function is obtained when the linearized hydrodynamics is modified to include Gaussian viscoelasticity and compressibility. The hydrodynamic friction on the bond appears to agree qualitatively very well, although quantitative agreement is not found at high frequencies. Various limits of the hydrodynamic friction are discussed. © *1995 American Institute of Physics.*

I. INTRODUCTION

The generalized Langevin equation[1,2] (GLE) is frequently used to calculate rate constants and vibrational relaxation times. In this formalism, the solvent degrees of freedom are eliminated from the nonequilibrium thermodynamic description with the help of the Mori–Zwanzig projection operator technique[3] to find a set of stochastic integro-differential equations for dynamical state of the solute. For example, the GLE for the displacement of of a particle of mass m along the x direction is

$$m\ddot{x}=-\frac{\partial\Phi(x)}{\partial x}-\int_0^t d\tau\zeta(t-\tau)\dot{x}(\tau)+F(t), \tag{1}$$

where $F(t)$ is the random force, $\zeta(t)$ is the dynamic friction, k_B is the Boltzmann's constant, T is the absolute temperature, and $\Phi(x)$ is the potential surface on which the vibrational displacement moves. The random force has the following properties:

$$\langle F(t)\rangle=0, \tag{2}$$

$$\langle F(0)F(t)\rangle=k_BT\zeta(t). \tag{3}$$

Equation (3) is the second fluctuation-dissipation theorem which gives an explicit connection between the dynamic friction and the autocorrelation function of the random force. The GLE has been rigorously derived only for the case when the bath is assumed to be a collection of harmonic oscillators and the system-bath coupling is linear in the bath coordinates. Recent work has generalized this harmonic bath model to space and time dependent friction. In such cases, further appropriate generalizations of the GLE are required and, at present, this remains an open problem.

In order to use the GLE, one must know the dynamic friction as a function of time. Unfortunately, in most problems of physical interest, $\zeta(t)$ is not known although it is possible to determine it from molecular dynamics simulations as has been done for the friction on a single bond of simple molecules (e.g., the covalent bond of a diatomic molecule and the C–Cl stretch in CH_3Cl). In this paper we calculate the dynamic friction coefficient on such a bond from the equations of linearized hydrodynamics with appropriate boundary conditions.[4]

In the hydrodynamic model, the exact many-body dynamics of the solute-solvent system is replaced by a single mole interacting with a continuum fluid described by the Navier–Stokes equations of fluid mechanics. The interaction of the single molecule with the rest of the system is contained in a set of physically realizable boundary conditions on the surface of the body. The detailed description of the fluid mechanical system is determined by the context of the problem.

The earliest application of hydrodynamics to explain molecular relaxation phenomena is the Stokes–Einstein theory of the translational diffusion coefficient in a fluid. Einstein showed that the diffusion coefficient of a spherical body of radius R in a fluid with viscosity η is given by

$$D=\frac{k_BT}{\zeta}, \tag{4}$$

where ζ is the translational friction coefficient. Stokes calculated the drag force on a sphere moving with constant velocity in an incompressible fluid by solving the linearized Navier–Stokes equation and found, for stick boundary conditions,

$$\zeta=6\pi\eta R \tag{5}$$

and for slip boundary conditions,

$$\zeta=4\pi\eta R. \tag{6}$$

The Stokes–Einstein approximation for the diffusion coefficient is a very good approximation if the mass of the sphere is much larger than those of the molecules comprising the fluid medium, so that the motion of the sphere is supposedly steady. When the mass of the sphere is comparable to that of the surrounding molecules, the motion of the sphere is inherently unsteady, and it seems quite natural to generalize the friction to be time dependent. The first attempt to include the effect of unsteady motion was done by Boussinesq who generalized the Stokes calculation by deriving the drag force on a spherical particle executing harmonic oscillation in a vis-

 0021-9606/95/103(3)/1160/15/$6.00

cous incompressible fluid. The velocity correlation function (VCF) corresponding to a frequency dependent friction coefficient[4]

$$\frac{\langle v(0)v(t)\rangle}{\langle v(0)v(0)\rangle}=\frac{2}{\pi}\,\mathrm{Re}\int_0^\infty d\omega\,\frac{\cos\,\omega t}{-i\omega+\zeta(\omega)/m}, \tag{7}$$

based on the Boussinesq frequency dependent friction, was seen not to agree with Rahman's molecular dynamic experiments.[5] It was realized that on the time scale for molecular translational motion, the fluid behaves viscoelastically and the effects of compressibility are important. Zwanzig and Bixon[4] modified the hydrodynamic equations in order to incorporate unsteady motion of the molecular system. They demonstrated that simple hydrodynamic models can successfully describe the full time dependence of the velocity correlation function. Zwanzig and Bixon (ZB) calculated the frequency dependent friction by solving the linearized hydrodynamic equations for a spherical particle executing nonuniform translational motion in a compressible viscoelastic fluid with general stick-slip boundary conditions. While not in quantitative agreement, this model reproduces the qualitative features of the VCF in a Lennard-Jones fluid.[5] In addition, ZB obtained the asymptotic long time tail in the VCF of an atom in a simple fluid as a natural consequence of the hydrodynamic theory, in agreement with that observed by Alder and Wainwright.[6] Ernst *et al.*[7] have shown that the longest lived $t^{-3/2}$ term in the VCF of an atom in a simple fluid is independent of fluid structure and depends only on the hydrodynamic properties of the fluid. It was shown later by Levesque *et al.*[8] that the agreement of the Zwanzig–Bixon theory with the computer results is improved if the frequency dependent shear viscosity determined from molecular dynamics simulations by calculating the transverse current fluctuation is used instead of assuming a simple Maxwellian model.

It is more difficult to calculate the friction coefficient for a molecular bond than for the translational motion of an atom,[4] and whole body rotations of rigid molecules with simple[9,10] and more complex shapes.[11] Berne and Harp have proposed a method of calculating the dynamic friction on single spheres using molecular dynamics method.[12] Recently, more extensive molecular dynamic (MD) calculations for the friction on the bond have been done.[13–15] For example, if we consider a homonuclear diatomic molecule of reduced mass μ, the GLE for the intramolecular degree of freedom x can be written as

$$\mu\ddot{x}=-\frac{\partial W(x)}{\partial x}-\int_0^t\zeta_x(t-\tau)\dot{x}(\tau)d\tau+F(t), \tag{8}$$

where $W(x)$ is the potential of mean force and $\zeta_x(t)$ is the dynamic friction on the bond.

$$\zeta_x=\frac{[\zeta_{11}-\zeta_{12}]}{2}=\frac{[\zeta_{22}-\zeta_{21}]}{2}. \tag{9}$$

Here ζ_{11} is the friction on atom a_1 when atom a_1 is moving and atom a_2 is at rest, and ζ_{12} is the friction on atom a_1 when atom a_2 is in motion and atom a_1 is at rest. In the free draining model of bond friction, the cross terms are omitted. This approximation should be valid only when the two atoms are well separated. In this free draining limit, the friction on the bond ζ_x is half the friction on the single atom. The free-draining limit has been used to model friction on internal bonds.

(i) The linear hydrodynamic theory was applied to the vibrational relaxation (dephasing and population relaxation) by Metiu *et al.*[16] They model the diatomic as a spherocylinder vibrating along the cylinder axis. They do not calculate the velocity field set up by the oscillating sphero-cylinder but instead argue that since there is no fluid in between the two hemispherical extremities, the friction experienced by each hemispherical cap (and thus, the friction on the bond) is half that of the friction experienced by an oscillating sphere in unbounded fluid. This is true only when the bondlength is very large and the cross terms are negligible. This free draining limit ignores the detailed effect of the molecular structure on the friction. Metiu *et al.* also considered a breathing sphere model, but the quantitative conclusions derived from this model are the same.

(ii) Smith and Harris[17,18] have used molecular dynamics simulations to calculate the total force autocorrelation function for a single atom and relate this to the friction coefficient by using the second fluctuation dissipation theorem. They then take the friction on the bond to be half the value calculated for that of the single atom; that is, they invoke the free draining limit even when the two atoms are close to each other (small bond lengths). They also use an autoregressive procedure to model the dynamic friction for single atom.

In this paper we extend the linear hydrodynamic theory to the calculation of dynamic friction on the intramolecular vibrational degree of freedom of a diatomic molecule. We report a calculation of the dynamic friction on the bond of a homonuclear diatomic molecule. We do not invoke the free-draining approximation.

Our calculations are based on the full effect due to the motion of the total body in the fluid continuum. When the bond length is small, the molecule is modeled as an almost spherical axisymmetric quadrupole (deformed sphere model). For large bondlengths, the molecule is modeled as two spheres oscillating along the axis of symmetry (analogous to two dipoles radiating in a dispersive medium), hereafter called the two sphere model. In the hydrodynamic theory, the local interactions between the atoms are averaged by a set of boundary conditions on the surface of the atom and, as a consequence, one finds an unphysical cusp in the graph of the VCF at short times, rather than a smooth parabolic behavior. We observe that the deformed sphere model does not show a long-time tail in the VCF, whereas that of the two sphere model does. In molecular dynamic experiments, the forces vary continuously in space and time. The friction coefficient calculated thus differs from the hydrodynamic friction coefficients since, in these theories, the forces are essentially impulsive.[19] Following Madden, we subtract the contribution due to impulsive collisions at high frequencies from the hydrodynamic friction for comparison to MD results. The simple Maxwellian approximation of the viscoelastic model used in the earlier hydrodynamic theories does not suffice to produce the correct frequency dependence

of the friction and the power spectrum when compared to the MD results. We use Gaussian models with single relaxation times for the bulk viscosity and with two relaxation times for the shear viscosity. These results are compared to some of the molecular dynamic calculations done recently on a simple liquid system[13–15] and the agreement is been found to be good.

II. HYDRODYNAMIC MODEL

The motion in an infinite fluid medium is governed by the basic classical laws of conservation: the continuity equation (the conservation of mass), the force equation (the conservation of momentum), and the heat-exchange equation (the conservation of energy). Since it is assumed that the velocity, density, and pressure changes induced by a moving atom in the fluid are small, these equations may be linearized with respect to them. The velocity of the particle is an arbitrary function $\mathbf{U}(t)$ of time. This can be Fourier analyzed into frequency components $\mathbf{U}_\omega$,

$$\mathbf{U}(t)=\int_{-\infty}^{\infty} d\omega\ \mathbf{U}_\omega e^{-i\omega t} \tag{10}$$

as can be the frictional force $\mathbf{F}(t)$:

$$\mathbf{F}(t)=\int_{-\infty}^{\infty} d\omega\ \mathbf{F}_\omega e^{-i\omega t}. \tag{11}$$

Because of the linearity of the equations and the boundary conditions involved, we may solve the differential equations with the boundary conditions for each Fourier component individually. The compressibility condition (finite speed of sound propagation) requires that the divergence of the velocity vector be nonzero. The viscoelastic behavior of the fluid is accounted for by using complex frequency-dependent viscosity coefficients. For example, one can adopt Maxwell's form for the longitudinal and shear viscosities

$$\eta_l(\omega)=\frac{\eta_{l0}}{1-i\omega\tau_l} \tag{12}$$

and

$$\eta_s(\omega)=\frac{\eta_{s0}}{1-i\omega\tau_s}, \tag{13}$$

where η_{l0} and η_{s0} are the corresponding zero-frequency viscosities and τ_l and τ_s are the corresponding viscoelastic relaxation times.

It should be noted that, at the frequencies of interest here, the fluid is expected to behave isothermally, so that the temperature gradient is neglected and the gradient of the pressure is

$$\boldsymbol{\nabla} P=\frac{\partial P}{\partial \rho}\,\boldsymbol{\nabla}\rho=C^2\boldsymbol{\nabla}\partial\rho, \tag{14}$$

where C is the isothermal speed of sound in the fluid at a given temperature and density.

The usual linearized Navier–Stokes equation along with the continuity equation and the velocity of sound relation for isothermal case can be transformed into a single vector-Helmholtz equation, the detailed derivation of which can be found in the paper by Zwanzig and Bixon,[4]

$$c_l^2\boldsymbol{\nabla}\boldsymbol{\nabla}\cdot\mathbf{v}(\omega)-c_t^2\boldsymbol{\nabla}\times\boldsymbol{\nabla}\times\mathbf{v}(\omega)+\omega^2\mathbf{v}(\omega)=0, \tag{15}$$

where

$$c_l^2=C^2-\frac{i\omega\eta_l(\omega)}{\rho_0} \tag{16}$$

and

$$c_t^2=-\frac{i\omega\eta_s(\omega)}{\rho_0} \tag{17}$$

are the speeds of the longitudinal and the transverse waves, respectively, ρ_0 is the equilibrium density, and ω is the frequency of the Fourier-component of the velocity of the sphere. Alternatively, by Helmholtz's theorem[20] the solution can be written as the sum of the longitudinal velocity $\mathbf{v}_\parallel(\omega)$ and the transverse velocity $\mathbf{v}_\perp(\omega)$, having wave numbers k_l $(=\omega/c_l)$ and k_t $(=\omega/c_t)$, respectively, such that,

$$\boldsymbol{\nabla}^2\mathbf{v}_\parallel(\omega)+k_l^2\mathbf{v}_\parallel(\omega)=0 \tag{18}$$

and

$$\boldsymbol{\nabla}^2\mathbf{v}_\perp(\omega)+k_t^2\mathbf{v}_\perp(\omega)=0, \tag{19}$$

with the conditions

$$\boldsymbol{\nabla}\times\mathbf{v}_\parallel(\omega)=0 \tag{20}$$

and

$$\boldsymbol{\nabla}\cdot\mathbf{v}_\perp(\omega)=0. \tag{21}$$

The physical meaning of $\mathbf{v}_\parallel$ and $\mathbf{v}_\perp$ becomes obvious if one takes the spatial Fourier transform: $\mathbf{v}_\parallel$ is along the $\mathbf{k}$ vector and $\mathbf{v}_\perp$ is perpendicular to it.[20]

The stress tensor is written as

$$\tilde{\sigma}(\omega)=\eta_s(\omega)\left(2-\frac{c_l^2}{c_t^2}\right)\boldsymbol{\nabla}\cdot\mathbf{v}(\omega)+\eta_s(\omega)[\boldsymbol{\nabla}\mathbf{v}(\omega)+\mathbf{v}(\omega)\boldsymbol{\nabla}], \tag{22}$$

where η_s is the shear viscosity of the fluid. The boundary conditions on the surface are the kinematic condition,

$$[\mathbf{v}(\omega)-\mathbf{U}(\omega)]\cdot\hat{\mathbf{n}}=0, \tag{23}$$

the general slip condition,

$$\hat{\mathbf{n}}\cdot\tilde{\sigma}(\omega)\cdot\hat{\mathbf{t}}=\frac{\beta_{\text{slip}}}{R}\,[\mathbf{v}(\omega)-\mathbf{U}_\omega]\cdot\hat{\mathbf{t}}, \tag{24}$$

and the radiation condition,

$$\lim_{r\to\infty} v(\omega)=0, \tag{25}$$

where β_{slip} $(0\leqslant\beta_{\text{slip}}<\infty)$ is the coefficient of slip, $\hat{\mathbf{n}}$ and $\hat{\mathbf{t}}$ are the normal and the tangential unit vectors, respectively, and $\mathbf{U}_\omega$ is the velocity on the surface of the sphere. When $\beta_{\text{slip}}=0$, the fluid slips perfectly over the boundary and for $\beta_{\text{slip}}=\infty$, it sticks perfectly to the boundary. At the molecular level, the slip boundary condition has been found to be more appropriate.

The hydrodynamic force exerted on the surface of the sphere is obtained by integrating the stress tensor over the surface of the sphere,

$$\mathbf{F}_\omega = \oint_{\text{sphere}} \tilde{\sigma}_\omega \cdot d\mathbf{s} = -\zeta(\omega)\cdot \mathbf{U}_\omega . \tag{26}$$

Henceforth, in this paper, we shall be working with the Fourier components of the unsteady variables and so, the subscript ω will be suppressed.

A. Solution of the vector-Helmholtz equation in spherical coordinates

The vector-Helmholtz equation with the boundary conditions [(1.9)–(1.11)] defined on the surface of a sphere is separable in spherical coordinates in the sense of Helmholtz's theorem for vector fields,[20] and the general solution in terms of the spherical vector wave functions can be written as

$$\mathbf{v} = \sum_{\sigma nm} A^L_{\sigma nm}\mathbf{L}_{\sigma nm} + A^M_{\sigma nm}\mathbf{M}_{\sigma nm} + A^N_{\sigma nm}\mathbf{N}_{\sigma nm} . \tag{27}$$

$\mathbf{L}_{\sigma nm}$ is the longitudinal component

$$\mathbf{L}_{\sigma nm} = k_l^{-1}\boldsymbol{\nabla}[Y_{\sigma nm} h_n(k_l r)], \tag{28}$$

and $\mathbf{M}_{\sigma nm}$ and $\mathbf{N}_{\sigma nm}$ are the transverse components

$$\mathbf{M}_{\sigma nm} = \boldsymbol{\nabla}\times[\mathbf{r} Y_{\sigma nm} h_n(k_t r)], \tag{29}$$

$$\mathbf{N}_{\sigma nm} = k_t^{-1}\boldsymbol{\nabla}\times\mathbf{M}_{\sigma nm} . \tag{30}$$

These are written in terms of the solutions of the scalar Helmholtz equation in spherical coordinate system, $Y_{\sigma nm} h_n(kr)$, with $Y_{\sigma nm}$ being the spherical harmonic of order (n,m) and parity σ, and $h_n(kr)$ being the spherical Bessel function of the third kind of order n, also known as spherical Hankel function. Since we will consider problems involving only axisymmetric cases here, m will be zero throughout, and thus parity will then be redundantly even. Moreover, there is no contribution from the torsional component $\mathbf{M}_{\sigma nm}$, as we do not expect any ϕ component in the solution. The vectors $\mathbf{L}_n$ ($\mathbf{L}_{e,n0}$) and $\mathbf{N}_n$ ($\mathbf{N}_{e,n0}$) will then be simplified as

$$\mathbf{L}_n = \hat{r}\,\frac{dh_n(k_l r)}{d(k_l r)}\,P_n(\cos\,\theta) - \hat{\theta}\,\frac{h_n(k_l r)}{k_l r}\,P_n^1(\cos\,\theta), \tag{31}$$

$$\mathbf{N}_n = \hat{r} n(n+1)\,\frac{h_n(k_t r)}{k_t r}\,P_n(\cos\,\theta) - \hat{\theta}\,\frac{1}{k_t r}\,\frac{dh_n(k_l r)}{d(k_t r)}\,P_n^1(\cos\,\theta). \tag{32}$$

Aforementioned expressions for $\mathbf{L}$ and $\mathbf{N}$ have singularities at the origin and thus are the representations of the outgoing waves, as required by the radiation boundary condition. The corresponding expressions for the incoming waves involve Bessel functions,

$$\mathbf{l}_n = \hat{r}\,\frac{dj_n(k_l r)}{d(k_l r)}\,P_n(\cos\,\theta) - \hat{\theta}\,\frac{j_n(k_l r)}{k_l r}\,P_n^1(\cos\,\theta), \tag{33}$$

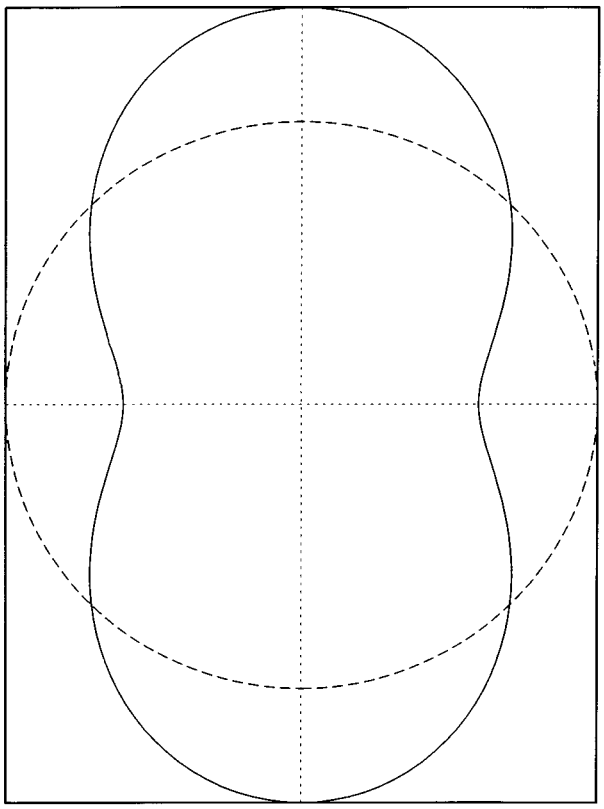

FIG. 1. Deformed sphere as a model to fit the description of a homonuclear diatom when the bondlength is small. $r = 1 + 2\epsilon\cos^2\theta - x\epsilon$ as referenced to $r = 1$.

$$\mathbf{n}_n = \hat{r} n(n+1)\,\frac{j_n(k_t r)}{k_t r}\,P_n(\cos\,\theta) - \hat{\theta}\,\frac{1}{k_t r}\,\frac{dj_n(k_l r)}{d(k_t r)}\,P_n^1(\cos\,\theta). \tag{34}$$

Thus, for the axisymmetric case, the velocity field for the outgoing wave is written as

$$\mathbf{v} = \sum_n A_n^L\mathbf{L}_n + A_n^N\mathbf{N}_n . \tag{35}$$

We find the coefficients A_n^L and A_n^L with the help of the boundary conditions [Eqs. (23)–(25)].

B. Flow due to the surface oscillation of a deformed sphere

When the bondlength of the homonuclear diatomic molecule is small, the surface of the diatom can be thought of as an axisymmetric perturbation to a sphere (see Fig. 1). Its surface is assumed to vibrate axisymmetrically so that the center of mass is fixed. Let the surface of the perturbed sphere be

$$r = a(1 + 2\epsilon\,\cos^2\,\theta) - x\epsilon \tag{36}$$

in spherical coordinates with its origin at the center of the undeformed sphere of radius a, $\epsilon(\leqslant 1)$ is a dimensionless parameter and x is the bondlength of the diatom. The term $2a\epsilon\cos^2\theta$ perturbs the sphere to a family of approximate

spheroids and $x\epsilon$ further distorts this to produce the notch in the diatom. The parameters r and ϵ are chosen to fit the diatom such that

$$R+x=a(1+2\epsilon)-x\epsilon$$

and

$$R=\max(r\ \cos\ \theta), \tag{37}$$

where R is the radius of the atoms.

The Fourier component of the velocity of the surface is,

$$\mathbf{U}_\omega=+U_0\hat{z} \quad \text{for } z\geqslant 0,$$

$$\mathbf{U}_\omega=-U_0\hat{z} \quad \text{for } z<0 \tag{38}$$

which in terms of the Legendre polynomials, can be written as

$$\mathbf{U}_\omega=U_0\hat{z}[\tfrac{3}{2}\ P_1(\cos\ \theta)-\tfrac{7}{8}\ P_3(\cos\ \theta)+\tfrac{11}{15}\ P_5(\cos\ \theta)-\cdots]. \tag{39}$$

We consider the solution for the perfect slip case [$\beta_{\text{slip}}=0$ in Eq. (24)], the perfect slipping boundary condition being more appropriate at the molecular level. Happel and Brenner[21] have described a method for calculating the velocity field for deformed spheres for time-independent flow. They make use of the Taylor series expansion about the undeformed sphere. We extend their method to the time dependent problem here in order to avoid divergences at high frequencies, since the special functions require careful consideration for their asymptotic behavior. The velocity field $\mathbf{v}$ is assumed to have an expansion of the form

$$\mathbf{v}=\sum_{n=0}^{\infty}\ \epsilon^n\mathbf{v}^{(n)}, \tag{40}$$

where each $\mathbf{v}^{(n)}$ satisfies the vector-Helmholtz equation

$$c_l^2\nabla\nabla\cdot\mathbf{v}^{(n)}-c_t^2\nabla\times\nabla\times\mathbf{v}^{(n)}+\omega^2\mathbf{v}^{(n)}=0. \tag{41}$$

This can be verified by direct substitution of the expansion in the vector-Helmholtz equation [Eq. (15)] and then equating terms involving like powers of ϵ. The radiation condition [Eq. (25)] gives, for each $\mathbf{v}^{(n)}$,

$$\lim_{r\to\infty}\mathbf{v}^{(n)}=0 \quad \text{for all } n=0,1,2,3,\ldots\ . \tag{42}$$

Each of the $\mathbf{v}^{(n)}$'s in the axisymmetric case has the form

$$\mathbf{v}^{(n)}(\mathbf{R}=\mathbf{r}[1+\epsilon f(a,\theta)])=\sum_k\ A_k^{(n)}\mathbf{L}_k(\mathbf{R})+B_k^{(n)}\mathbf{N}_k(\mathbf{R}) \tag{43}$$

with $f(a,\theta)=(2\cos^2\theta-x/a)$. To satisfy the boundary conditions, we expand the $\mathbf{v}^{(n)}$'s about $r=a$ by use of the translational properties of spherical waves (see the Appendix). The expansions for $\mathbf{L}\{R=r[1+\epsilon f(a,\theta)]\}$ and $\mathbf{N}\{R=r[1+\epsilon f(a,\theta)]\}$ in terms of $\mathbf{L}(r)$ and $\mathbf{N}(r)$ are

$$\mathbf{L}_n(R)=\sum_{m=0}^{\infty}\ T_{mn}^{(L)}[k_l r\epsilon f(a,\theta)]\mathbf{L}_m(r),$$

$$\mathbf{N}_n(R)=\sum_{m=0}^{\infty}\ T_{mn}^{(N)}[k_t r\epsilon f(a,\theta)]\mathbf{N}_m(r), \tag{44}$$

where $T_{mn}^{(L)}[k_l r\epsilon f(a,\theta)]$ and $T_{mn}^{(N)}[k_t r\epsilon f(a,\theta)]$ are functions of the spherical Bessel functions rather than the spherical Hankel functions since $|\epsilon f(a,\theta)|<1$. Using the product theorem of Bessel functions,[22] we can write

$$\frac{j_l[kr\epsilon f(a,\theta)]}{[\epsilon f(a,\theta)]^l}=\frac{2}{kr}\sum_{s=0}^{\infty}\ \frac{(2s+l+\frac{3}{2})\Gamma(s+l+\frac{3}{2})}{\Gamma(l+\frac{3}{2})s!}\ {}_2F_1(-s,l+s+3/2,l+3/2;[\epsilon f(a,\theta)]^2)j_{l+2s+1}(kr), \tag{45}$$

where ${}_2F_1(-s,l+s+3/2,l+3/2;[\epsilon f(a,\theta)]^2)$ is the confluent hypergeometric function with argument $[\epsilon f(a,\theta)]^2$.

Calculation to zero-order is easily done by using unperturbed vector waves to satisfy the boundary conditions on the unperturbed sphere. For higher order terms, we substitute these expansions in the kinetic boundary condition [cf. Eq. (23)] and the general boundary condition [cf. Eq. (24)] with $\beta_{\text{slip}}=0$ on the surface of the undeformed sphere and then equate terms involving like powers of ϵ to get the perturbation of the $\mathbf{v}$ field.

In order to calculate the friction opposing the motion of the perturbed sphere in the $\hat{z}$ direction, we note that the differential force exerted on the surface in $\mathbf{z}$ direction on a differential area element $d\Omega$ is

$$\frac{d}{d\Omega}\ \mathbf{F}\cdot\hat{z}=\hat{z}\cdot\tilde{\sigma}\cdot\mathbf{n}=\sigma_{rr}\cos\ \theta \quad \text{on } r=a \tag{46}$$

which implies that the differential drag $d\zeta/d\Omega$ exerted on the area element $d\Omega$ having surface velocity $U_0\mathbf{z}$ is

$$\frac{d\zeta}{d\Omega}=-\frac{\sigma_{rr}\cos\ \theta}{U_0} \quad \text{on } r=a. \tag{47}$$

The friction on the surface above the xy plane is found by integrating over the surface ($r=a, 0\leqslant\theta<\pi/2, 0\leqslant\phi<2\pi$)

$$\zeta_{(0\leqslant\theta\leqslant\pi/2)}=-\int_0^{\pi/2}\int_0^{2\pi}\ \frac{\sigma_{rr}}{U_0}\ a^2\ \sin\ \theta\ \cos\ \theta d\ \theta d\ \phi \tag{48}$$

$$=-2\pi a^2\int_0^{\pi/2}\ \frac{\sigma_{rr}}{U_0}\sin\ \theta\ \cos\ \theta\ d\theta. \tag{49}$$

Similarly, on the surface below the xy plane

$$\zeta_{(-\pi/2\leqslant\theta\leqslant 0)}=-2\pi a^2\int_{-\pi/2}^{0}\ \frac{\sigma_{rr}}{U_0}\sin\ \theta\ \cos\ \theta\ d\theta. \tag{50}$$

Since xy plane is the plane of symmetry with respect to the boundary conditions, we must have

$$\zeta_{(0\leqslant\theta\leqslant\pi/2)}=\zeta_{(-\pi/2\leqslant\theta\leqslant 0)}. \tag{51}$$

We calculate the approximate friction $\zeta_{(0\leqslant\theta\leqslant\pi/2)}$ only to first order, since the algebra becomes tremendously involved:

$$\zeta_{(0\leqslant\theta\leqslant\pi/2)}=\frac{\pi a\eta_s}{2}\left[\left(4-\frac{x^2}{(1-iy)}\right)\left(1+\frac{\alpha\epsilon}{3}+O(\epsilon^2)\right)-\frac{25\beta}{32}\right] \tag{52}$$

with

$$x=k_t a,\quad h_{nt}=h_n(x),\quad y=k_l a,$$

$$h_{nl}=h_n(y),\quad \alpha=\left(3\gamma+\frac{25}{4}\frac{N}{\delta}\right),$$

$$N=\left(\frac{h_{2t}}{x}(16-x^2)-2h_{1t}\right)\left[\tfrac{3}{5}\Phi(y)\left(2h_{0l}-4\frac{h_{1l}}{y}-3h_{2l}+12\frac{h_{3l}}{y}\right)\right]-\frac{12}{5x}(h_{1l}-4h_{3l})[\tfrac{3}{5}\Phi(x)(2h_{1t}-3h_{3t})-h_{2t}],$$

$$\delta=\left(2h_{1l}h_{3t}+3h_{3l}h_{1t}-\frac{xh_{2t}}{2}(2h_{1l}-3h_{3l})\right),$$

$$\gamma=\Phi(y)(-y^2-2iy+2)/(1-iy),$$

$$\beta=N_1/\delta,$$

$$N_1=16h_{1l}\left(2\frac{h_{2t}}{x}-h_{1t}\right)-xh_{2t}\left(\frac{h_{2l}}{y}(40-x^2)-4h_{1l}\right)+2(24+x^2)h_{1t}\frac{h_{2l}}{y},$$

$$\Phi(\alpha)=\frac{1}{\alpha}\left(\frac{j_1[\alpha\epsilon f(a,\theta)]}{\epsilon f(a,\theta)}\right)\Bigg|_{\epsilon^0} \tag{53}$$

from Eq. (45).

To find the relation between the bond friction ζ_x [c.f. Eq. (9)] and $\zeta_{(0\leqslant\theta\leqslant\pi/2)}$, we recognize that

$$\zeta_{11}-\zeta_{12}=\zeta_{(0\leqslant\theta\leqslant\pi/2)} \tag{54}$$

is the friction on one of the faces due to the combined motion of both of the faces, one motion opposing the other. Thus, the friction on the bond is

$$\zeta_x=\frac{\zeta_{(0\leqslant\theta\leqslant\pi/2)}}{2} \tag{55}$$

for the deformed sphere model.

C. Flow due to oscillations of two spheres along the line joining them

When the bondlength of a real diatomic molecule is sufficiently large (about twice the Lennard-Jones radius), it is possible that a solvent atom can enter into the neck. Then the single deformed sphere model does not suffice to describe the diatom and one can think of the molecule as consisting of two spherical atoms, so that fluid is allowed to penetrate the region between the two atoms. The friction experienced by each sphere is not only due to its own motion but also due to the motion of the other sphere close enough to sufficiently affect the total friction experienced by each of them [cf. Eq. (9)]. This cross effect has been ignored in earlier models.[16,18] We calculate in this section the dynamic friction experienced by each of the spheres when they are oscillating with a phase difference of π.

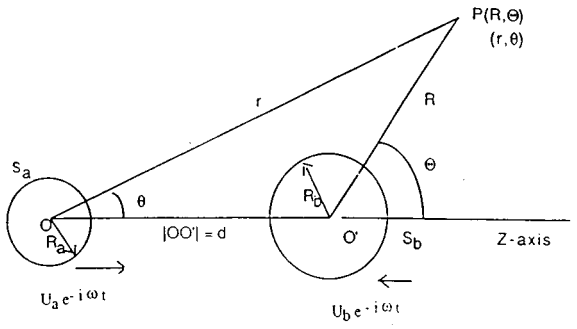

FIG. 2. Coordinates for two spheres oscillating along their axis of symmetry with infinitesimal amplitude.

It is not so difficult to obtain an exact solution for the friction for either stick or slip boundary condition when time dependence is ignored since then the biharmonic equation satisfied by the stream function is separable in the bispherical coordinate system.[23] Whereas, for the case of a time dependent problem, the vector-Helmholtz equation is not separable in the bispherical coordinate system. We exploit the linearity of the differential equation and the boundary conditions and utilize the method of superposition of fields about two centers to obtain the approximate solution.

Let a sphere S_a of radius R_a have its center at origin O and a sphere S_b of radius R_b have its center at O' situated a distance d away on the z axis (see Fig. 2). Let a point $P(\mathbf{r},\mathbf{R})$ have coordinates (r,θ,ϕ) and (R,Θ,Φ) with respect to origins O and O' in spherical coordinate systems.

The solution for the two-center linear-field problem can be written as the linear combination of the fields about different centers

$$\mathbf{V}(\mathbf{r},\mathbf{R})=\mathbf{v}(\mathbf{r})+\mathbf{v}'(\mathbf{R}), \tag{56}$$

where the fields $\mathbf{v}(\mathbf{r})$ and $\mathbf{v}(\mathbf{R})$ can be written as linear combinations of the spherical vector-wave functions about centers O and O'. Thus

$$\mathbf{V}(\mathbf{r},\mathbf{R})=\sum_n\left[A_n^L\mathbf{L}_n(\mathbf{r})+A_n^N\mathbf{N}_n(\mathbf{r})\right]+\sum_n\left[B_n^L\mathbf{L}_n(\mathbf{R})+B_n^N\mathbf{N}_n(\mathbf{R})\right]. \tag{57}$$

In order to satisfy the boundary conditions on S_a and S_b, one needs to expand $\mathbf{L}_n$ and $\mathbf{N}_n$ into multipole fields about different centers. We derive their translational properties in the Appendix. The expansions for $\mathbf{L}$ and $\mathbf{N}$ about O' in terms of $\mathbf{l}$ and $\mathbf{n}$ about O are

$$\mathbf{L}_n(\mathbf{R})=\sum_{m=0}^{\infty} T'^{(L)}_{mn}(k_l d)\mathbf{l}_m(\mathbf{r}),$$
$$\mathbf{N}_n(\mathbf{R})=\sum_{m=0}^{\infty} T'^{(N)}_{mn}(k_t d)\mathbf{n}_m(\mathbf{r}), \tag{58}$$

and the corresponding expansions for $\mathbf{L}$ and $\mathbf{N}$ about O in terms of $\mathbf{l}$ and $\mathbf{n}$ about O' are

$$\mathbf{L}_n(\mathbf{r})=\sum_{m=0}^{\infty} T^{(L)}_{mn}(k_l d)\mathbf{l}_m(\mathbf{R}),$$
$$\mathbf{N}_n(\mathbf{r})=\sum_{m=0}^{\infty} T^{(N)}_{mn}(k_t d)\mathbf{n}_m(\mathbf{R}). \tag{59}$$

With these expansions, we can write the field about center O as

$$\mathbf{V}(\mathbf{r})=\sum_{n=0}^{\infty} A^L_n\mathbf{L}_n(\mathbf{r})+A^N_n\mathbf{N}_n(\mathbf{r})+\sum_{n=0}^{\infty}\sum_{m=0}^{\infty} B^L_n T'^{(L)}_{mn}(k_l d)\times\mathbf{l}_m(\mathbf{r})+B^N_n T'^{(N)}_{mn}(k_t d)\mathbf{n}_m(\mathbf{r}). \tag{60}$$

Similarly, about center O', the field is

$$\mathbf{V}(\mathbf{R})=\sum_{n=0}^{\infty}\sum_{m=0}^{\infty} A^L_n T^{(L)}_{mn}(k_l d)\mathbf{l}_m(\mathbf{R})+A^N_n T^{(N)}_{mn}(k_t d)\times\mathbf{n}_m(\mathbf{R})+\sum_{n=0}^{\infty} B^L_n\mathbf{L}_n(\mathbf{R})+B^N_n\mathbf{N}_n(\mathbf{R}). \tag{61}$$

Since dipole–dipole (and induced dipole–dipole) interactions dominate, we shall keep only the $n=1$ and $m=1$ term. Then the representation of fields about two centers are

$$\mathbf{V}(\mathbf{r})=A^L_1\mathbf{L}_1(\mathbf{r})+A^N_1\mathbf{N}_1(\mathbf{r})+B^L_1 T'^{(L)}_{11}(k_l d)\mathbf{l}_1(\mathbf{r})+B^N_1 T'^{(N)}_{11}(k_t d)\mathbf{n}_1(\mathbf{r}), \tag{62}$$

$$\mathbf{V}(\mathbf{R})=A^L_1 T^{(L)}_{11}(k_l d)\mathbf{l}_1(\mathbf{R})+A^N_1 T^{(N)}_{11}(k_t d)\mathbf{n}_1(\mathbf{R})+B^L_1\mathbf{L}_1(\mathbf{R})+B^N_1\mathbf{N}_1(\mathbf{R}). \tag{63}$$

Let us look at the expression for the force experienced by the sphere S_a in the z direction,

$$\mathbf{F}_{S_a}\cdot\hat{z}=2\pi R_a^2\int_0^{\pi}\sin\theta(\sigma_{rr}\cos\theta-\sigma_{r\theta}\sin\theta)d\theta. \tag{64}$$

σ_{rr} and $\sigma_{r\theta}$ depend on θ as $P_n(\cos\theta)$ and $P^1_n(\cos\theta)$, respectively. Integration over the range $(0,\pi)$ is nonzero only when n is equal to one. Furthermore, the expansion of $\mathbf{v}'(\mathbf{R})$ about the origin O is regular inside S_a (Bessel functions being regular at $r=0$), and thus cannot produce a resultant force on S_a.[21] Hence, we only need to know the coefficients $A^{(L)}_1$ and $A^{(N)}_1$ for the calculation of the friction on the sphere S_a. As most of the contributions comes from the interaction between the dipolar terms ($n=1$ and $m=1$ terms) of the expansion, we retain only these terms for the calculation of coefficients. Therefore, the expression for the field about O and O' becomes

$$\mathbf{V}(\mathbf{r})=A^{(L)}_1\mathbf{L}_1(\mathbf{r})+A^{(N)}_1\mathbf{N}_1(\mathbf{r})+B^{(L)}_1 T'^{(L)}_{11}(k_l d)\mathbf{l}_1(\mathbf{r})+B^{(N)}_1 T'^{(N)}_{11}(k_t d)\mathbf{n}_1(\mathbf{r}),$$
$$\mathbf{V}(\mathbf{R})=A^{(L)}_1 T^{(L)}_{11}(k_l d)\mathbf{l}_1(\mathbf{R})+A^{(N)}_1 T^{(N)}_{11}(k_t d)\mathbf{n}_1(\mathbf{R})+B^{(L)}_1\mathbf{L}_1(\mathbf{R})+B^{(N)}_1\mathbf{N}_1(\mathbf{R}). \tag{65}$$

Consider the case when the two spheres have equal radii $R_a=R_b=R$ and their Fourier components of the velocities are $U\mathbf{z}$ and $-U\mathbf{z}$. Symmetry of the problem about xy plane requires that

$$A^{(L)}_1=-B^{(L)}_1,$$
$$A^{(N)}_1=-B^{(N)}_1. \tag{66}$$

We also note that for $n=m=1$,

$$T^{(L)}_{11}(k_l d)=T'^{(L)}_{11}(k_l d),$$
$$T^{(N)}_{11}(k_t d)=T'^{(N)}_{11}(k_t d). \tag{67}$$

Now, the velocity field about center O satisfies a much simplified equation which must be solved to calculate the friction on sphere S_a, namely,

$$\mathbf{V}(\mathbf{r})=A^{(L)}_1[\mathbf{L}_1(\mathbf{r})-T^{(L)}_{11}(k_l d)\mathbf{l}_1(\mathbf{r})]+A^{(N)}_1[\mathbf{N}_1(\mathbf{r})-T^{(N)}_{11}(k_t d)\mathbf{n}_1(\mathbf{r})] \tag{68}$$

with the boundary conditions on S_a,

$$\mathbf{v}\cdot\hat{n}=U\cos\theta,$$
$$\sigma_{r\theta}=\frac{\beta_{\text{slip}}}{R}(\mathbf{v}\cdot\hat{t}+U\sin\theta),$$
$$\lim_{r\to\infty}\mathbf{v}=0. \tag{69}$$

We calculate the velocity $\mathbf{V}(\mathbf{r})$ from the above equations. The friction is calculated from the stress tensor in the integral in Eq. (64). The value of friction on sphere S_a then is

$$\zeta_a=4\pi R\eta_s\left[A^{(L)}\left(\frac{k_t}{k_l}\right)^2 k_l R h_{1l}+2A^{(N)}k_t R h_{1t}\right] \tag{70}$$

with

$$x=k_t R,$$
$$h_{nt}=h_n(x),$$
$$y=k_l R,$$
$$h_{nl}=h_n(y),$$
$$A^{(L)}=\frac{1}{\Delta}\left[\left(h_{2t}-\frac{xh_{1t}}{2+(\beta_{\text{slip}}/\eta_s)}\right)-\left(j_{2t}-\frac{xj_{1t}}{2+(\beta_{\text{slip}}/\eta_s)}\right)\times\left(\frac{3h_1(k_t d)}{k_t d}\right)\right],$$
$$A^{(N)}=\frac{1}{\Delta}\{[h_{2l}-j_{2l}(h_0(k_l d)-2h_2(k_l d)]\}, \tag{71}$$

and

$$\Delta=\Delta_1+\Delta_2-\Delta_3-\Delta_4,$$

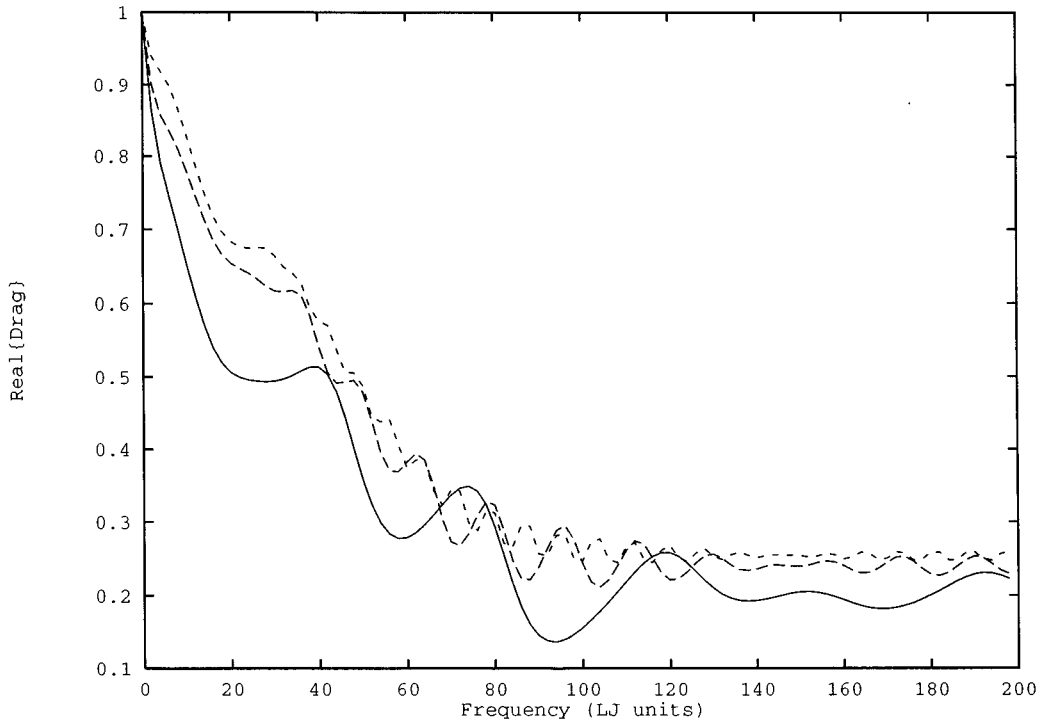

FIG. 3. Real part of friction for the two sphere model as a function of frequency for different distances between the spheres with fixed radii. Solid line, $d=2.1\sigma$; dashed lines, $d=5.0\sigma$; dashed small lines, $d=10.0\sigma$.

$$\Delta_1=\{2h_{2l}h_{0t}+h_{0l}h_{2t}+[xh_{1t}/(2+\beta_{\rm slip}/\eta_s)]\times(2h_{2l}-h_{0l})\},$$

$$\Delta_2=3[h_0(k_ld)-2h_2(k_ld)]\left(\frac{h_1(k_td)}{k_td}\right)\left(2j_{2l}j_{0t}+j_{0l}j_{2t}+\frac{xj_{1t}}{2+(\beta_{\rm slip}/\eta_s)}(2j_{2l}-j_{0l})\right),$$

$$\Delta_3=[h_0(k_ld)-2h_2(k_ld)]\left(2j_{2l}h_{0t}+j_{0l}h_{2t}+\frac{xh_{1t}}{2+(\beta_{\rm slip}/\eta_s)}(2j_{2l}-j_{0l})\right),$$

$$\Delta_4=3\left(\frac{h_1(k_td)}{k_td}\right)\left(2h_{2l}j_{0t}+h_{0l}j_{2t}+\frac{xj_{1t}}{2+(\beta_{\rm slip}/\eta_s)}\times(2h_{2l}-h_{0l})\right). \tag{72}$$

The expression for $\zeta_a(\omega)$ can be written as a linear combination of e^{ik_ld} and ϵ^{ik_td} and thus one observes oscillations in the real and the imaginary parts of friction as a function of frequency. As the distance between the spheres increases, the amplitude of the oscillation and the period decrease in magnitude. This behavior is characteristic of the viscoelastic modeling and is absent when the fluid is not viscoelastic. Such oscillations are not found in the molecular dynamics simulations. These oscillations are due to the unphysical nature of the boundary conditions at finite frequencies. Moreover, the hydrodynamic equations describe collective motions of long wavelength. Figure 3 shows the real part of friction as a function of frequency for different sphere separation d, with fixed r with a Gaussian model of viscoelasticity instead of the Maxwell form (see comparison with MD results).

In the limit of bondlength going to infinity, the terms containing Hankel functions with arguments k_ld and k_td go to zero. Thus, we get

$$\zeta_{\rm sp}=\lim_{d\to\infty}\zeta_a=\frac{4\pi R\eta_s}{\Delta_\infty}\left[\left(h_{2t}-\frac{xh_{1t}}{2+(\beta_{\rm slip}/\eta_s)}\right)\left(\frac{x^2}{y}\right)h_{1l}+2h_{2l}xh_{1t}\right], \tag{73}$$

where

$$\Delta_\infty=\left(2h_{2l}h_{0t}+h_{0l}h_{2t}+\frac{xh_{1t}}{2+(\beta_{\rm slip}/\eta_s)}(2h_{2l}-h_{0l})\right) \tag{74}$$

which is the result obtained by Zwanzig and Bixon for a single sphere in an unbounded fluid.[16]

The dynamic friction ζ_a (Eq. 70) can be related to the bond friction in Eq. (9) by recognizing that

$$\zeta_{11}-\zeta_{12}=\zeta_a. \tag{75}$$

Thus we find,

$$\zeta_x=\frac{\zeta_a}{2} \tag{76}$$

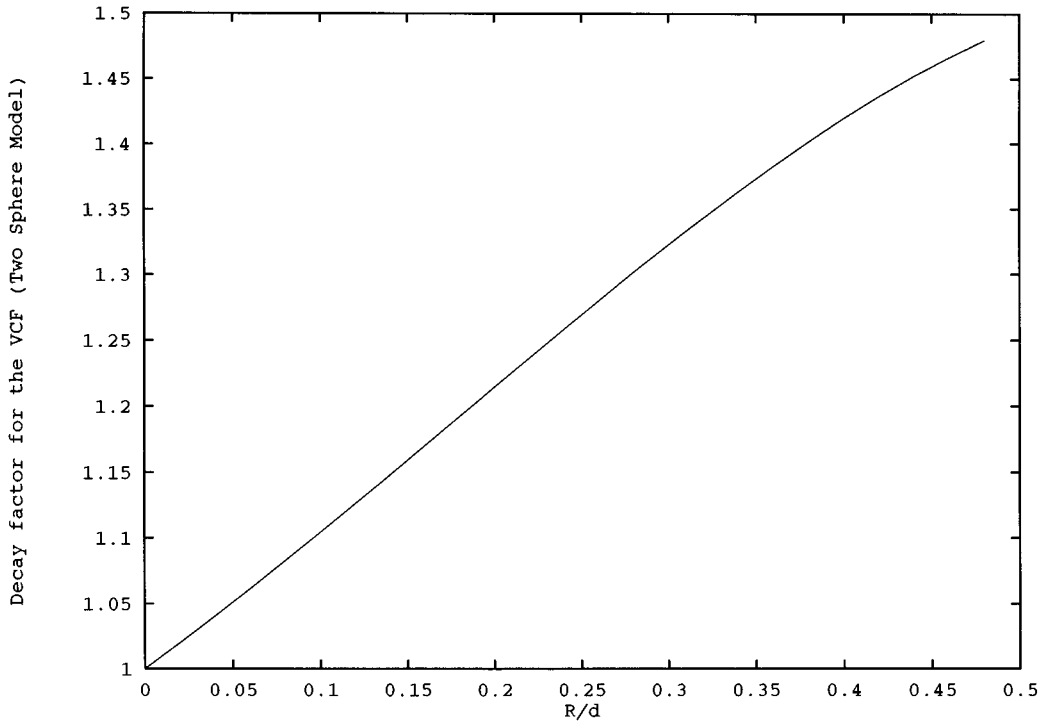

FIG. 4. Decay factor for the velocity correlation function [Eq. (85)] as a function of R/d, the ratio of atomic radius and bond-length for the two sphere model.

for the two-sphere model. If the two atoms are well separated ($d\to\infty$), the cross frictions ($\zeta_{12}=\zeta_{21}$) are almost zero. Then, the friction on the bond is equal to

$$\lim_{d\to\infty}\zeta_x=\zeta_{\rm sp}/2. \tag{77}$$

$\zeta_{\rm sp}$ is the friction experienced by single sphere in absence of the other sphere [see Eq. (73)].

D. Limiting behavior of friction

1. Low frequency behavior

The relation between the velocity correlation function and the frequency dependent friction[4] is

$$\frac{\langle v(0)v(t)\rangle}{\langle v(0)v(0)\rangle}=\frac{2}{\pi}\,\mathrm{Re}\int_0^\infty d\omega\,\frac{\cos\,\omega t}{-i\omega+\zeta_x(\omega)/\mu}. \tag{78}$$

Let us consider the deformed sphere model first. At very low frequencies, the friction on the bond, $\zeta_x(\omega)$, is linearly dependent on frequency,

$$\zeta_x(\omega)\sim a+b\omega+o(\omega^{3/2}). \tag{79}$$

Consequently, from Eq. (78),

$$\frac{\langle v(0)v(t)\rangle}{\langle v(0)v(0)\rangle}\sim a'\,\delta(t)+b'\,\frac{d}{dt}\,\delta(t)+\cdots \tag{80}$$

we see that, asymptotically, the VCF appears to have no long time tail, in contrast with the behavior reported by Alder and Wainwright[6] on hard spheres. For the two sphere model, at low frequencies, the expression for $\zeta_x(\omega)$ for the perfect slip case ($\beta_{\rm slip}=0$) turns out to be

$$\zeta_x(\omega)\sim 2\pi R\eta_s\Big((1-\alpha)+\frac{1}{3}\,(\alpha+(R/d)^2-2)\times\frac{1+i}{(2\eta_s)^{1/2}}\,(\rho_0\omega)^{1/2}\Big), \tag{81}$$

where

$$\alpha=2(R/d)-2(R/d)^2+(R/d)^3-\tfrac{1}{5}(R/d)^6. \tag{82}$$

Thus, in this case, the VCF has a $t^{-3/2}$ long-time tail:

$$\frac{\langle v(0)v(t)\rangle}{\langle v(0)v(0)\rangle}\sim\frac{\mu}{4R\rho_0}\,\frac{[2-\alpha-(R/d)^2]}{3(1-\alpha)}\left(\frac{\eta_s\pi t}{\rho_0}\right)^{-3/2}. \tag{83}$$

In the limit of bondlength going to infinity, the VCF decays as

$$\lim_{d\to\infty}\frac{\langle v(0)v(t)\rangle}{\langle v(0)v(0)\rangle}\sim\frac{\mu}{6R\rho_0}\left(\frac{\eta_s\pi t}{\rho_0}\right)^{-3/2} \tag{84}$$

as noted by Zwanzig and Bixon for a single sphere case.[4]

As we know, the long time tail in the VCF of an unbound particle arises from the convective motion in the fluid set by an unsteadily moving sphere. The fluid elements in front of the sphere move out and to the back so as to enforce the motion of the sphere in its own direction of movement. This is also true when we have two spheres, only now the enforcement gets enhanced by a factor which is dependent on the distance between the spheres. Intuitively, we can think of replacing one of the spheres by a wall in front of the other sphere which pushes the fluid in front of the sphere to the back more efficiently,

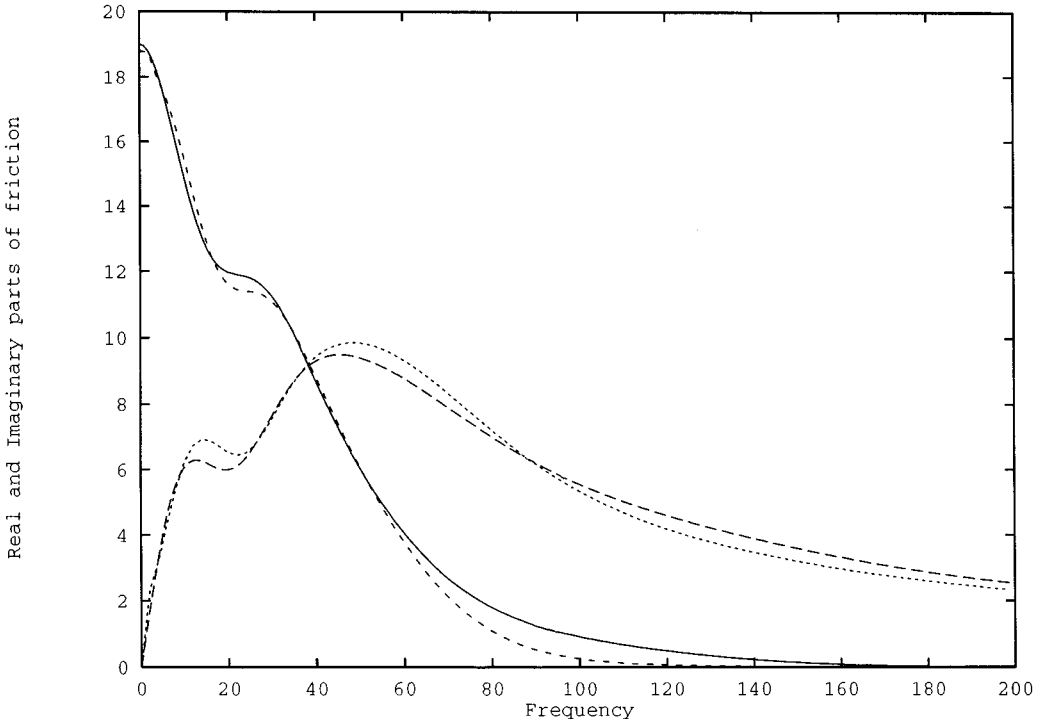

FIG. 5. Real and Imaginary parts of frequency dependent friction for single solvent atom at $\hat{\rho}=1.05$ compared to analytic fit from the MD experiment of Straub *et al.* (Ref. 15) for the same case. Solid and dashed lines, the real and the imaginary parts from MD; diamonds and crosses, the real and the imaginary parts, respectively, from hydrodynamic theory [Eq. (77)].

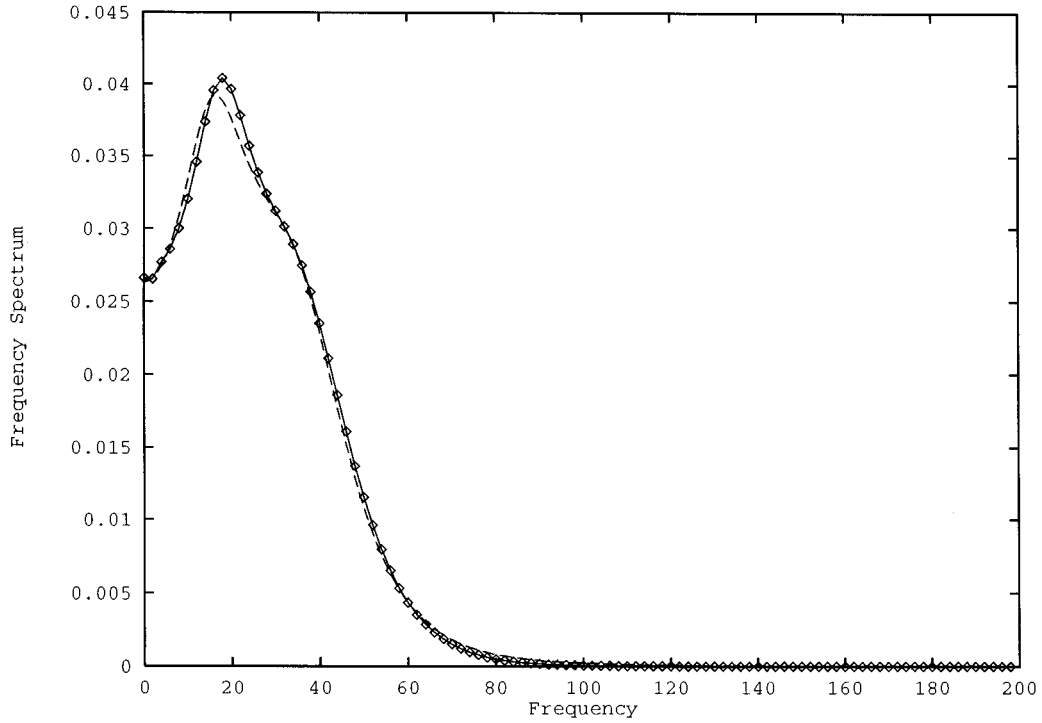

FIG. 6. Frequency spectrum of the velocity correlation function for single solvent atom at $\hat{\rho}=1.05$ compared to analytic fit from the MD experiment of Straub *et al.* (Ref. 15) for the same case reported in Ref. 13. Broken line, MD; diamonds, hydrodynamic theory.

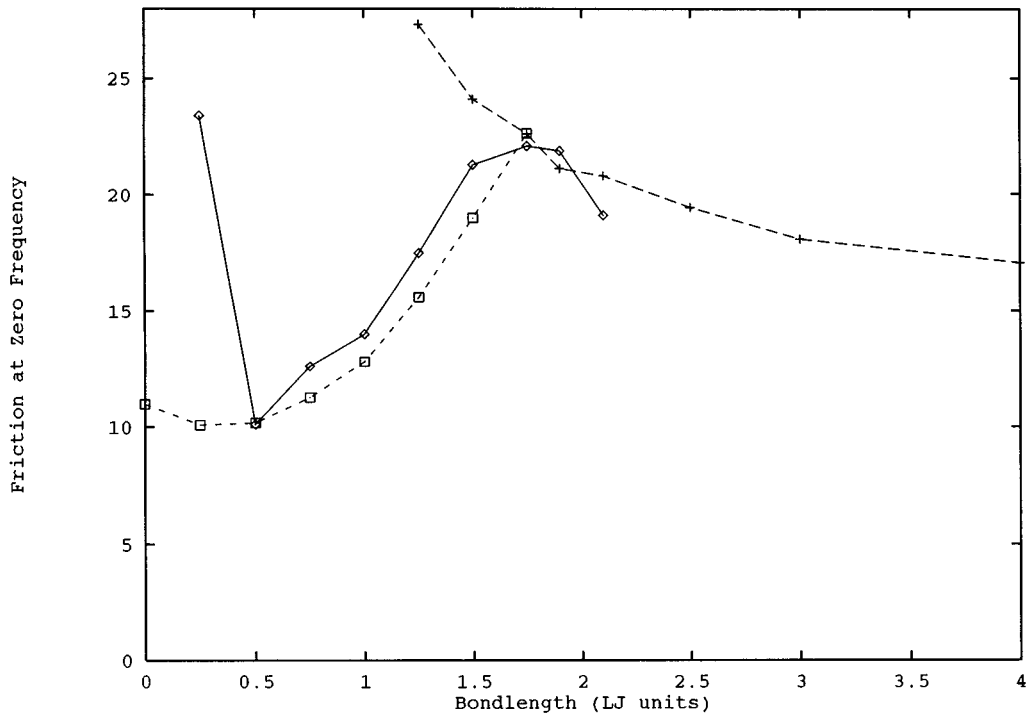

FIG. 7. Comparison of zero frequency value of the bond friction as a function of the bondlength, $\zeta_{\text{bond}}(\omega=0)$ of a diatom. Hydrodynamic calculation vs the molecular dynamics result obtained by Straub *et al.* (Ref. 14). Diamonds, Straub *et al.* (Ref. 14), boxes, deformed sphere model; crosses, two sphere model.

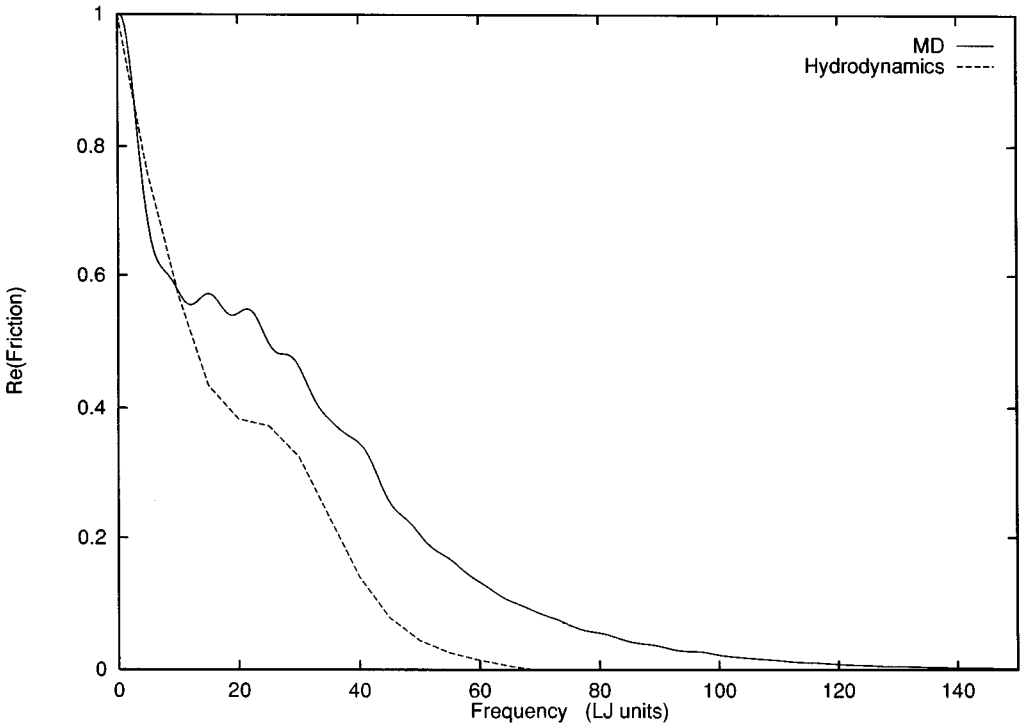

FIG. 8. Comparison of real part of the frequency dependent friction on the bond at bondlength $x=1.25$ LJ units for $\hat{\rho}=1.05$. Hydrodynamic calculation vs the molecular dynamics result obtained by Berne *et al.* (Ref. 13) Bold line, MD result; thin line, hydrodynamic result.

$$\langle v(0)v(t)\rangle \sim \frac{[2-\alpha-(R/d)^2]}{2(1-\alpha)} \lim_{d\to\infty}\langle v(0)v(t)\rangle. \tag{85}$$

This enhanced factor has been plotted against the ratio R/d in Fig. 4. The factor is a monotonically increasing function of R/d and is maximum when R/d is maximum (touching case). In the case of the deformed sphere model, no fluid can penetrate between the two lobes of the diatom. As a consequence, one does not see any enforcing convective behavior and there will be no long time tail.

2. High frequency behavior

In real molecular fluids with continuous forces

$$\lim_{\omega\to\infty} J_x(\omega)=0. \tag{86}$$

In contrast, in hydrodynamic calculations the high frequency friction is nonzero. For example, in the case of the two sphere model, when $\omega\to\infty$, the real part of friction on the bond approaches a finite value,

$$\lim_{\omega\to\infty}\zeta_x(\omega)=2\pi R^2\rho_0\,\frac{(c_l^{(\infty)}+2c_t^{(\infty)})}{3}, \tag{87}$$

where for the perfect stick case

$$\begin{aligned} c_l^{(\infty)}&=c_l(\omega\to\infty),\\ c_t^{(\infty)}&=c_t(\omega\to\infty). \end{aligned} \tag{88}$$

A similar argument is applicable for the deformed sphere model.

At short times in real fluids the local interactions become important and the boundary conditions in the hydrodynamic description do not take these interactions into account. At very short times, if we apply kinetic theory of gases and calculate the pressure exerted by an ideal gas having the speed of sound $c_{\rm av}=(c_l^{\infty}+2c_t^{\infty})/3$ and density ρ_0 on a macroscopic sphere of radius R, it is easy to see that this pressure is proportional to the limiting value of the friction calculated in Eq. (87). However, kinetic theory based on hard sphere interactions also has discontinuities.

III. COMPARISON WITH MOLECULAR DYNAMICS RESULTS

Recently, the dynamic friction on the bond of a diatomic molecule in a heat bath of argon atoms has been calculated using the molecular dynamic method.[13–15] The frequency dependent friction and the frequency spectrum of the velocity correlation function as functions of bondlength have been reported. In Sec. II, we derived the expression for the dynamic friction on the bond using the equations of linearized hydrodynamics with the more realistic slip boundary condition appropriate at the molecular level for the distorted-sphere [cf. Eq. 52 with Eq. (55)] and two-sphere [cf. Eq. (70) with Eq. (76)] models for small and large bondlengths, respectively. We now compare our hydrodynamic results to molecular dynamic simulations of a diatomic molecule dissolved in a simple fluid.

In the earlier hydrodynamic models for calculating the frequency dependent friction coefficient,[4,8] the Maxwell's form of viscoelasticity [cf. Eqs. (12) and (13)] has been used. We find that the important structural features at finite frequencies in the atomic friction obtained [Eq. (76)] are absent (see Ref. 13, Fig. 6) if we use the simple Maxwell form of viscoelasticity with four adjustable parameters for the shear and the bulk viscosities $\eta_s(t)$ and $\eta_l(t)$. Since it is known that the Gaussian forms best describe the qualitative nature of relaxation of the shear and the bulk viscosities in the simple liquids,[8] we anticipated that missing structural features might be recovered if we use a more realistic Gaussian model instead. After trying various combinations of Maxwell and Gaussian forms, we find that the following form with six adjustable parameters seems to be best:

$$\begin{aligned} \eta_s(t)&=\eta_s(0)[\exp(-t^2/\tau_{s1}^2)+(\alpha_s t)^4\,\exp(-t^2/\tau_{s2}^2)],\\ \eta_l(t)&=\eta_l(0)\exp(-t^2/\tau_l^2). \end{aligned} \tag{89}$$

The Laplace transform of these Gaussians involve Fresnel's integral and we do the transform numerically. In the MD experiments, the forces considered are smooth functions of space and time and purely impulsive collisions are not present. In contrast, in the hydrodynamic theory, the forces are impulsive.[19] Thus, to reduce our expressions for the frequency dependent friction to those of the MD simulations at high frequencies, we subtract the impulsive part [which is constant and real in the limit of infinite frequency, c.f. Eq. (87)] from the total frequency dependence

$$\zeta_{\rm bond}(\omega)=\zeta_x(\omega)-\zeta_x(\infty). \tag{90}$$

First we fit our single particle friction ($d\to\infty$ in the expression for the friction on the bond from the two sphere model, Eq. 70) to the MD results given by Straub *et al.*[15] Straub's analytic fit to the time dependent single particle friction obtained from MD is numerically fourier transformed to get the real and imaginary parts of frequency dependent friction and the frequency spectrum of the velocity correlation function at reduced densities $\hat{\rho}=1.05$ and 1.0 and the reduced temperature $\hat{T}=2.5$. We need to adjust the seven parameters (the zero frequency values of the Laplace-transformed viscosities and their relaxation parameters, η_{l0}, η_{s0}, τ_l, τ_{s1}, τ_{s2}, α_s and the velocity of sound C) required to described the continuum fluid. The radius of the atom is taken to be $\sigma/2$, where σ is the LJ diameter of an argon atom ($\sigma=0.3504$ nm). Since a large number of parameters are needed to fit the curves, there is no straightforward way to fit them except by trial and error. However, to begin with, the reasonable guess is the one reported by Metiu *et al.*[16] The maxima and minima in these curves are fit by varying the relaxation parameters. The velocity of sound affects the fit only in the low frequencies region. We also keep in mind the fact that η_{l0} can be no less than $4\eta_{s0}/3$, an important requirement which follows from hydrodynamics. Once we have obtained these parameters for best fit for a certain density, they are used to calculate the friction on the bond at that density for both models (the distorted sphere model and the two sphere model). The values of these parameters at the reduced density $\hat{\rho}=1.05$ are found to be

$$\eta_{l0}=10.6\times10^{-3}\ \text{P},$$
$$\eta_{s0}=6.91\times10^{-3}\ \text{P},$$
$$\tau_{s1}=1.11\times10^{-13}\ \text{s},$$
$$\tau_{s2}=2.36\times10^{-13}\ \text{s}, \tag{91}$$
$$\tau_{l}=2.35\times10^{-13}\ \text{s},$$
$$\alpha_{s}=2.71\times10^{12}\ \text{s}^{-1},$$
$$c=8.0\times10^{4}\ \text{cm/s},$$

and at $\hat{\rho}=1.0$,

$$\eta_{l0}=8.69\times10^{-3}\ \text{P},$$
$$\eta_{s0}=5.45\times10^{-3}\ \text{P},$$
$$\tau_{s1}=1.11\times10^{-13}\ \text{s},$$
$$\tau_{s2}=2.36\times10^{-13}\ \text{s}, \tag{92}$$
$$\tau_{l}=2.36\times10^{-13}\ \text{s},$$
$$\alpha_{s}=2.57\times10^{12}\ \text{s}^{-1},$$
$$c=7.0\times10^{4}\ \text{cm/s}.$$

We show the comparison plots for the real and imaginary parts of the friction on the bond for the case of the free draining limit at $\hat{\rho}=1.05$ in Fig. 5. Figure 6 shows the corresponding frequency spectrum of the velocity correlation function [the integrand in Eq. (78)]. It can be seen that we recover the missing structural features of the frequency dependent friction at finite frequencies for the case of free draining by using the Gaussian form for viscoelasticity. The static friction ($\omega\rightarrow0$ value) for different bondlengths at $\hat{\rho}=1.0$ is compared to the results of Straub *et al.*[14] in Fig. 7. The maximum in the zero frequency friction occurs at a bondlength of about 1.7 LJ units where the deformed sphere model breaks down. The bondlength is sufficiently large so that atoms can move into the neck of the diatom, then the two sphere model becomes more appropriate. The comparison plot for bondlength $x=1.25$ LJ units for the real part of friction as reported in the paper by Berne *et al.*[13] is given in Fig. 8. At this bondlength, the distorted sphere model should be appropriate as can be seen from the static friction plot (Fig. 7). Qualitative, but not quantitative, agreement is found especially at high frequencies. The molecular dynamic friction is found to decay slower than the hydrodynamic friction. The large disagreement at high frequencies may be attributed to the absence of high frequency modes in the hydrodynamic model which does not include the molecular level interaction in the boundary conditions. The same can be concluded from the two sphere model. In Fig. 3 we observe oscillations at high frequencies. This is due to reflection of sound waves between the boundaries of finitely separated spheres. The amplitudes of these trapped waves become smaller as the separation between the spheres grows. Thus, the two sphere model also fails to correctly describe high frequency behavior for large bondlengths.

IV. CONCLUSION

Linearized hydrodynamic theory has been used to study rotational line shapes, dynamics of polymers and atomic diffusion with fair degree of success, which motivated us to use this simple theory to do the calculation of the dynamic friction on the bond of a diatomic molecule. There already exists an attempt to compute this function using molecular hydrodynamics based on the free draining limit.[16] Berne and co-workers[13–15] have shown from molecular dynamics that the free draining limit is not valid for the treatment of diatomic molecules. They showed that the friction coefficient depends on bondlength. The purpose of this paper is to calculate the dynamic friction on the bond using more accurate boundary conditions. We have treated the hydrodynamic interaction between parts of the molecule using two different sets of boundary conditions:—a two sphere model and a deformed sphere model. Both of these models give dynamic friction coefficients that depend on bondlength. The static friction on the bond ($\omega\rightarrow0$) can be calculated within reasonable approximations using these models. However, at high frequencies (at short times) the linearized hydrodynamic theory departs from the computer results because of the unphysical nature of the hydrodynamic boundary conditions. The two sphere model shows unphysical oscillations at finite frequencies, because the viscoelastic continuum penetrates the region between the two spheres. The deformed sphere model, however, does not show such undulations, because the continuum fluid cannot penetrate the diatomic molecule. Consequently, the deformed sphere model gives a qualitatively correct picture at all frequencies only after a correction [c.f. Eq. (90)] is made for the unphysical infinite frequency limit found in any hydrodynamic model. The Gaussian model for viscoelasticity is needed to correctly reproduce the friction calculated for a single atom at all frequencies. When this is done, the deformed sphere model predicts a dynamic friction on the bond in reasonable agreement with molecular dynamics.

The perturbation method for calculating the velocity vector used in the paper can easily be generalized to more complicated geometries to study low frequency, long wavelength molecular phenomena such as rotational dynamics or dynamics in polymers.

APPENDIX: TRANSLATIONAL PROPERTIES OF SPHERICAL VECTOR-WAVE FUNCTIONS

The translational properties of scalar and vector wave functions can be derived from the expansion formula for plane waves in spherical coordinates.[24,25] We report here the results with some details of derivation. The expansion formula for the plane wave in spherical wave about origin O (see Fig. 2) is

$$e^{i\mathbf{k}\cdot\mathbf{r}}=\sum_{n=0}^{\infty}\sum_{m=-n}^{n}4\pi i^{n}Y_{nm}^{*}(\theta',\phi')Y_{nm}(\theta,\phi)j_{n}(kr), \tag{A1}$$

where $\mathbf{k}$ has coordinates (k,θ',ϕ') about O and those of $\mathbf{r}$, (r,θ,ϕ). We start with the vector equation [with $\mathbf{R}$: (R,Θ,Φ), $\mathbf{d}$: (d,η,ψ), and $d>\max[r,R]$]

$$\mathbf{r}=\mathbf{R}+\mathbf{d}, \tag{A2}$$

and therefore,

$$e^{i\mathbf{k}\cdot\mathbf{r}}=e^{i\mathbf{k}\cdot\mathbf{R}}e^{i\mathbf{k}\cdot\mathbf{d}}. \tag{A3}$$

Then we have, using Eq. (74),

$$\sum_{lm} Y^*_{lm}(\theta',\phi')Y_{lm}(\theta,\phi)j_l(kr)=\sum_{Lm} Y^*_{LM}(\theta',\phi')Y_{LM}(\Theta,\Phi)j_L(kr)\sum_{\lambda\mu} Y^*_{\lambda\mu}(\theta',\phi')Y_{\lambda\mu}(\eta,\psi)j_\lambda(kr). \tag{A4}$$

Multiplying both sides by $Y_{lm}(\theta',\phi')$ and integrating over θ' and ϕ', we get

$$Y_{lm}(\theta,\phi)j_l(kr)=\sum_{\lambda,\mu}\sum_{Lm} 4\pi i^{\lambda+L-l}Y_{\lambda\mu}(\eta,\psi)j_\lambda(kd)Y_{LM}(\Theta,\Phi)j_L(kR)\int_0^\pi\int_0^{2\pi}\sin\theta'\,d\theta'\,d\phi' Y_{lm}(\theta',\phi')Y^*_{lm}(\theta',\phi')$$

$$=\sum_{LM} Y_{LM}(\Theta,\Phi)j_L(kR)[i^l S_{LM,lm}(kd,\eta,\psi)] \tag{A5}$$

with

$$S_{LM,lm}(kd,\eta,\psi)=\sum_{\lambda,\mu} 4\pi i^{\lambda+L-l}Y_{\lambda\mu}(\eta,\psi)j_\lambda(kd)(-1)^m[(2l+1)(2L+1)(2\lambda+1)]^{1/2}\begin{pmatrix} l & L & \lambda\\ 0 & 0 & 0\end{pmatrix}\begin{pmatrix} l & L & \lambda\\ -m & M & \mu\end{pmatrix} \tag{A6}$$

where

$$\begin{pmatrix} l & L & \lambda\\ -m & M & \mu\end{pmatrix}$$

is the Wigner 3-j symbol. It is noticed here that since k's in our case are complex numbers, the translational operators are no longer unitary.

When one considers the outgoing field $Y_{\lambda\mu}(\eta,\psi)h_l(kr)$ about the center O, in order to have correct convergence behavior, the expansion for $d>\max[r,R]$ is

$$Y_{lm}(\theta,\phi)h_l(kr)=\sum_{LM} Y_{LM}(\Theta,\Phi)j_L(kR)[i^l S_{LM,lm}(kd,\eta,\psi)] \tag{A7}$$

with

$$S_{LM,lm}(kd,\eta,\psi)=\sum_{\lambda,\mu} 4\pi i^{\lambda+L-l}Y_{\lambda\mu}(\eta,\psi)h_\lambda(kd)(-1)^m[(2l+1)(2L+1)(2\lambda+1)]^{1/2}\begin{pmatrix} l & L & \lambda\\ 0 & 0 & 0\end{pmatrix}\begin{pmatrix} l & L & \lambda\\ -m & M & \mu\end{pmatrix}. \tag{A8}$$

Then, for the longitudinal component of the wave-vector $\mathbf{L}_{lm}$, we have the expression

$$\mathbf{L}_{\sigma lm}(\mathbf{r})=k_l^{-1}\nabla[Y_{\sigma lm}h_l(k_l r)]=k_l^{-1}\sum_{LM}\nabla[Y_{LM}(\Theta,\Phi)j_L(k_l R)][i^l S_{LM,lm}(kd,\eta,\psi)]=\sum_{LM}[i^l S_{LM,nm}(k_l d,\eta,\psi)]\mathbf{L}_{\sigma LM}(\mathbf{R}). \tag{A9}$$

This follows from the fact that the gradient operator is invariant under coordinate transformation. For the torsional wave-vector component $\mathbf{M}_{lm}$, we have

$$\mathbf{M}_{\sigma lm}(\mathbf{r})=\nabla\times[\mathbf{r}Y_{\sigma lm}h_l(k_t r)]=\nabla[Y_{\sigma lm}h_l(k_t r)]\times\mathbf{r}=\sum_{LM}[i^l S_{LM,lm}(k_t d,\eta,\psi)]\nabla[Y_{LM}(\Theta,\Phi)j_L(k_t R)]\times(\mathbf{R}+\mathbf{d})$$

$$=\sum_{LM}[i^l S_{LM,lm}(k_t d,\eta,\psi)]\mathbf{M}_{LM}(\mathbf{R})+\sum_{LM}[i^l S_{LM,lm}(k_t d,\eta,\psi)]\nabla[Y_{LM}(\Theta,\Phi)j_L(k_t R)]\times\mathbf{d}. \tag{A10}$$

Because of the divergenceless condition, we can write relation (A10) as

$$\mathbf{M}_{\sigma lm}(\mathbf{r})=\sum_{LM}[\alpha_{LM,lm}(k_t d,\eta,\psi)\mathbf{M}_{\sigma LM}(\mathbf{R})+\beta_{LM,lm}(k_t d,\eta,\psi)\mathbf{N}_{LM}(\mathbf{R})]. \tag{A11}$$

As $\mathbf{N}\sim\nabla\times\mathbf{M}$ and $\mathbf{M}\sim\nabla\times\mathbf{N}$, we also have

$$\mathbf{N}_{\sigma lm}(\mathbf{r})=\sum_{LM}[\alpha_{LM,lm}(k_t d,\eta,\psi)\mathbf{N}_{\sigma LM}(\mathbf{R})+\beta_{LM,lm}(k_t d,\eta,\psi)\mathbf{M}_{LM}(\mathbf{R})], \tag{A12}$$

where $\alpha_{LM,lm}$ and $\beta_{LM,lm}$ can be evaluated in terms of the $S_{LM,lm}$. For the axisymmetric case, the expansions turn out to be

$$\mathbf{L}_l(\mathbf{r}) = = \sum_L T_{Ll}^{(L)}(k_l d)\mathbf{l}_L(R)] \tag{A13}$$

with

$$T_{Ll}^{(L)}(k_l d) = (2L+1) \sum_{\lambda=|l-L|}^{l+L} (-1)^{L+\lambda-l}(2\lambda+1) \times \begin{pmatrix} l & L & \lambda \\ 0 & 0 & 0 \end{pmatrix}^2 h_\lambda(k_l d) \tag{A14}$$

and

$$\mathbf{N}_l(\mathbf{r}) = = \sum_L T_{Ll}^{(N)}(k_t d)\mathbf{n}_L(R)] \tag{A15}$$

with

$$T_{Ll}^{(N)}(k_t d) = (2L+1)\frac{1}{2} \sum_{\lambda=|l-L|}^{l+L} (-1)^{L+\lambda-l}(2\lambda+1) \times [l(l+1)L(L+1)]^{-1/2} \times [l^2+l+L^2+L-(\lambda^2+\lambda)] \times \begin{pmatrix} l & L & \lambda \\ 0 & 0 & 0 \end{pmatrix}^2 h_\lambda(k_t d). \tag{A16}$$

For $l=L=1$, we have, for translation from O' to O,

$$\begin{aligned} T_{11}^{(L)}(k_l d) &= h_0(k_l d) - 2h_2(k_l d), \\ T_{11}^{(N)}(k_t d) &= h_0(k_t d) + h_2(k_t d). \end{aligned} \tag{A17}$$

For translation from O to O', we use the vector relation with $\mathbf{d} \rightarrow -\mathbf{d}$,

$$\mathbf{R} = \mathbf{r} - \mathbf{d}. \tag{A18}$$

One finds, for the axisymmetric case.

$$\begin{aligned} T_{Ll}'^{(L)}(k_l d) &= (-1)^{l+L} T_{Ll}^{(L)}(k_l d), \\ T_{Ll}'^{(N)}(k_t d) &= (-1)^{l+L} T_{Ll}^{(N)}(k_t d). \end{aligned} \tag{A19}$$

Thus, for $l=L=1$

$$\begin{aligned} T_{11}'^{(L)}(k_l d) &= T_{11}^{(L)}(k_l d), \\ T_{11}'^{(N)}(k_t d) &= T_{11}^{(N)}(k_t d). \end{aligned} \tag{A20}$$

[1] P. Hänggi, P. Talkner, and M. Borkovec, Rev. Mod. Phys. **62**, 250 (1990).
[2] B. J. Berne, M. Borkovec, and J. E. Straub, J. Phys. Chem. **92**, 3711 (1988).
[3] H. Mori, Prog. Theor. Phys. **33**, 433 (1965).
[4] R. Zwanzig and M. Bixon, Phys. Rev. A **2**, 2005 (1970).
[5] A. Rahman, Phys. Rev. A **136**, 405 (1964).
[6] B. J. Alder and T. E. Wainwright, Phys. Rev. **1**, 18 (1970).
[7] M. H. Ernst, E. H. Hague, and J. M. J. van Leeuwen, Phys. Rev. Lett. **25**, 1257 (1970).
[8] D. Levesque, L. Verlet, and J. Kürkijarvi, Phys. Rev. A **7**, 1690 (1973).
[9] B. J. Berne, J. Chem. Phys. **56**, 2164 (1972).
[10] C. Hu and R. Zwanzig, J. Chem. Phys. **60**, 4353 (1974).
[11] G. K. Youngren and A. Acrivos, J. Chem. Phys. **63**, 3846 (1975).
[12] B. J. Berne and G. D. Harp, Adv. Chem. Phys. **17**, 63 (1970).
[13] B. J. Berne, M. E. Tuckerman, J. E. Straub, and A. L. R. Bug, J. Chem. Phys. **93**, 5084 (1990).
[14] J. E. Straub, B. J. Berne, and B. Roux, J. Chem. Phys. **93**, 6804 (1990).
[15] J. E. Straub, M. Borkovec, and B. J. Berne, J. Chem. Phys. **89**, 4833 (1988).
[16] H. Metiu, D. W. Oxtoby, and K. F. Freed, Phys. Rev. A **15**, 361 (1977).
[17] D. E. Smith and C. B. Harris, J. Chem. Phys. **92**, 1304 (1990).
[18] D. E. Smith and C. B. Harris, J. Chem. Phys. **92**, 1312 (1990).
[19] A. J. Masters and P. A. Madden, J. Chem. Phys. **74**, 2450 (1981).
[20] P. M. Morse and H. Feshbach, *Methods Of Theoretical Physics* (McGraw Hill, New York, 1953).
[21] J. Happel and H. Brenner, *Low Reynolds Number Hydrodynamics* (Prentice Hall, Englewood Cliffs, NJ, 1965).
[22] G. N. Watson, *A Treatise on the Theory of Bessel Functions* (Cambridge University Press, New York, 1966).
[23] M. Stimson and G. B. Jeffery, Proc. R. Soc. London Ser. A **111**, 110 (1926).
[24] L. C. Maximon and M. Danos, J. Math. Phys. **6**, 766 (1965).
[25] W. C. Chew, *Waves And Fields In Inhomogeneous Media* (Van Nostrand Reinhold, New York, 1990).